J. Fluid Mech. (2010), *vol.* 645, *pp.* 529–539.
doi:10.1017/S0022112009993065

Quantitative measurement of the lifetime of localized turbulence in pipe flow

D. J. KUIK†, C. POELMA AND J. WESTERWEEL

Laboratory for Aero & Hydrodynamics, Delft University of Technology, Mekelweg 2, 2628 CD Delft, The Netherlands

(Received 22 July 2009; revised 26 October 2009; accepted 26 October 2009)

Transition to turbulence in a pipe is characterized by the increase of the characteristic lifetimes of localized turbulent spots ('puffs') with increasing Reynolds number (Re). Previous experiments are based on visualization or indirect measurements of the lifetime probability. Here we report quantitative direct measurements of the lifetimes based on accurate pressure measurements combined with laser Doppler anemometry (LDA). The characteristic lifetime is determined directly from the lifetime probability. It is shown that the characteristic lifetime does not diverge at finite Re, and follows an exponential scaling for the observed range $1725 \leqslant Re \leqslant 1955$. Over this small Re range the lifetime increases over four orders of magnitude. The results show that the puff velocity is not constant, and the rapid disintegration of puffs occurs within 20–70 pipe diameters.

1. Introduction

The transition to turbulence in pipe flow can be characterized by the lifetimes of localized turbulent spots or 'puffs'. These puffs co-exist with the laminar flow state, and travel downstream with a velocity of around the bulk velocity (Lindgren 1969; Wygnanski & Champagne 1973). Faisst & Eckhardt (2004) used a direct numerical simulation (DNS) to investigate the lifetime of the turbulent flow state in a short periodic pipe. They found that the probability $P(t; Re)$ of survival at a given Reynolds number (Re) decays exponentially with time, reminiscent of a memoryless process, i.e.

$$P(t; Re) = \exp[-(t - t_0)/\tau(Re)], \tag{1}$$

where t_0 represents a formation time of the disturbance, and $\tau(Re)$ the characteristic lifetime of the disturbances. Faisst & Eckhardt (2004) obtained $\tau(Re)$ from the median lifetime of the disturbances, which appeared to scale as $\tau^{-1} \propto (Re_c - Re)$, where Re_c is a *critical Reynolds number* at which the lifetime diverges. Earlier, new solutions of the Navier–Stokes equations for pipe flow, in the form of travelling waves, were identified (Faisst & Eckhardt 2003; Hof *et al.* 2004; Wedin & Kerswell 2004). These solutions were thought to form a *strange saddle* in phase space, so that a disturbance of the base flow, i.e. Hagen–Poiseuille flow that is represented as a stable node, leads to a transient for which the duration increases proportional to the Reynolds number. A divergence of the duration of the transient, or lifetime of the disturbance, that occurs

† Email address for correspondence: d.j.kuik@tudelft.nl

at finite Reynolds number implies a transition from a strange saddle to a strange attractor in phase space (Eckhardt *et al.* 2007). The strange attractor would implicate turbulence as a sustained flow state.

Faisst & Eckhardt (2004) found $Re_c \cong 2250$, which agrees with empirical data. However, re-examination of the data, where $\tau(Re)$ was evaluated directly from the slope of $P(t;Re)$ in a semilog plot, showed that $\tau(Re)$ scales exponentially, i.e. $\tau^{-1} \propto \exp(-Re)$, so that the lifetime does not diverge at a finite critical Reynolds number (Hof *et al.* 2006). To examine in which way the lifetime diverges with Re requires long observations times of several hundred or even thousands of integral time scales.

Peixinho & Mullin (2006) carried out an experiment to determine $P(t;Re)$ by observing the decay of a puff in a constant mass flux pipe. First, a puff was generated at $Re = 1900$, and when it had survived 100 pipe diameters the Reynolds number was reduced, and the decay of the puff was observed. The turbulent motion in the puff was visualized with small platelets, and the moment of decay was determined visually. The results confirmed the exponential probability in (1), and it was found that τ^{-1} scales linearly with $Re_c \cong 1750 \pm 10$. Willis & Kerswell (2007*a*) represented the experiment in a DNS. They also found an exponential distribution for $P(t;Re)$ and a linear scaling of τ^{-1}, although the observation times where rather short, with $Re_c \cong 1870$. However, re-evaluation of their data showed that the same results would be reconcilable with an exponential scaling of τ^{-1} (Hof *et al.* 2007; Willis & Kerswell 2007*b*). Recent data (Hof *et al.* 2008) showed that the lifetime scales super-exponentially, i.e. $\tau^{-1} \propto \exp[-(Re/c)^n]$ with $n = 9$ and $c = 1549$, over eight orders of magnitude in τ.

The measurements of $\tau(Re)$ by Hof *et al.* (2006, 2008) are based on the probability $P(Re;L)$ that a puff survives a given pipe length L as a function of Reynolds number. This probability has a characteristic S-shape in the case of an exponential scaling of $\tau(Re)$. However, this implicitly assumes that $P(t;Re)$ has the form given in (1). Also, this experiment does not allow to constantly monitor the formation of the puff after the injection, the motion of the puff along the pipe, and its sudden decay. Especially at high Reynolds number, where only a very small fraction of puffs decays before reaching the pipe exit, it is difficult to make a distinction between puffs that decay in the pipe and a possible misfiring of the disturbance mechanism or disturbances that failed to generate a puff. Furthermore, this approach requires an estimate of the mean puff velocity, in order to convert the distance L into a lifetime.

In this paper, we report results of quantitative lifetime measurements that are based on accurate pressure measurements. This makes it possible to directly determine $P(t;Re)$, rather than relying on an implicit assumption that the lifetime probability follows (1). Since we measure over a pipe section that excludes the injection it is possible to determine $\tau(Re)$ irrespective of the puff formation. The inlet length for laminar pipe flow at $Re = 2 \times 10^3$ is $\sim 120\ D$, so that any applied disturbances that failed to generate a puff are expected to have decayed before the first pressure tap at $L/D = 125$ (see § 2). Apart from being able to directly measure the lifetime t that individual puffs travel along the pipe, it is possible to determine the decay time during which the puff disintegrates. It is thus possible to validate the assumption of sudden puff decay that underlies the expression for $P(t;Re)$ in (1).

2. Experimental set-up and method

The flow facility used for the measurements is similar to the set-up used by Hof *et al.* (2006, 2008). Figure 1 shows a schematic overview of the set-up. The main difference

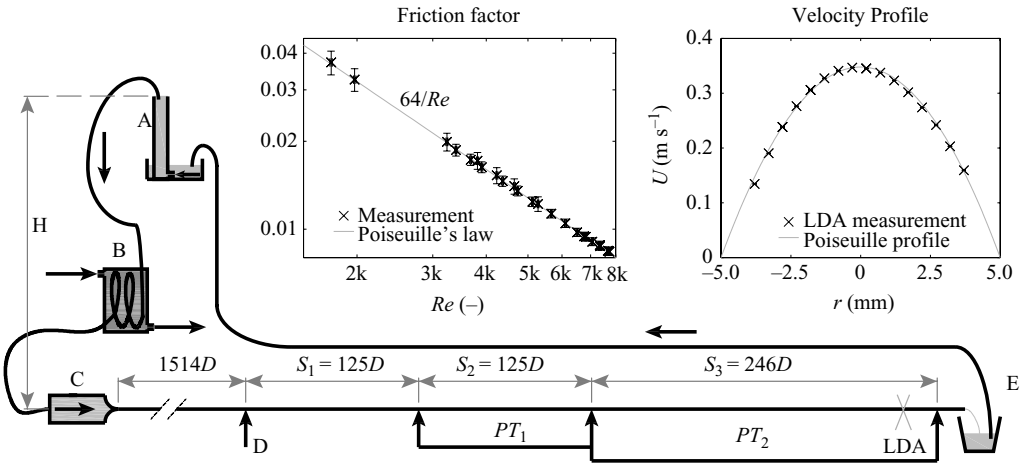

FIGURE 1. Schematic of the experimental set-up. A: overflow reservoir to maintain constant pressure head (H); B: heat exchanger; C: flow conditioner containing several meshes with reducing grid size and a smooth 1:100 area contraction; D: flow disturbance; E: pipe exit with second reservoir from which fluid is pumped back into reservoir (A); $PT_{1,2}$: pipe sections over which the pressure drop is measured by a pressure transducer. S: indicates a pipe section; laser Doppler anemometry (LDA): location of velocity measurement by LDA. Inset, left: measured friction factor (×) as a function of Reynolds number together with Poiseuille's friction law (—); error bars represent an estimate of the total experimental error. Inset, right: velocity profile measured with LDA (×) together with a calculated velocity profile based on the mass flow rate (—).

is that in the current set-up special care is taken to reduce pressure fluctuations. The 20 m long pipe is made of 16 glass tubes, each 120–130D in length, with an inner diameter of $D = 10 \pm 0.01$ mm. The pipe sections are joined by PMMA connectors with the same inner diameter, that contain 0.5 mm holes which could either be used for sensing the pressure or to introduce the flow disturbance. The water flow is driven by the constant pressure head generated by the height difference between the free surface of the overflowing reservoir (A) and the outflow of the pipe (E). At regular intervals the fluid from reservoir E is pumped back into the base from which the overflowing reservoir is fed. The flow rate of the system can be adjusted manually by changing the total pressure head between 3.0 and 3.5 m (corresponding to $30–35 \times 10^3$ Pa).

To reduce pressure fluctuations in the pipe, the amount of overflowing fluid has been minimized. Furthermore, the fluid was introduced from the bottom and guided through a set of flow straighteners to remove any remaining fluctuations caused by the pump and the introduction of the fluid into the reservoir. From the top reservoir, the fluid flows through a feeding line consisting of two segments: one 10 m long copper tubing segment and one 15 m long flexible tubing segment.

The 20 m pipe section is thermally insulated from the environment. To control the temperature of the working fluid, temperature-controlled water is forced around the copper segment (B), creating a heat exchanger by which the daily temperature variation is maintained to within $\pm 0.3\,^{\circ}$C. To determine the exact Reynolds number at which each measurement is taken, the temperature of the water is continuously monitored at the pipe exit (E) using a calibrated mercury thermometer. Using a digital camera, the temperature reading could be determined with a precision of $3.4 \times 10^{-3}\,^{\circ}$C.

The main pressure drop occurs between sections A and C, where the tube has a smaller diameter (6 mm) than in the straight pipe. In this section the flow remains turbulent, and the total pressure loss is much larger than in the 10 mm diameter pipe. Introduction of a turbulent disturbance in the pipe (D) lowers the flow rate by the additional friction of the local turbulent flow. However, one can easily verify that the flow rate changes by less than 0.01 % for the current configuration, because of the large pressure drop over the feeding line. Therefore this set-up can be considered to effectively operate with a constant mass flux condition. In a numerical investigation Willis & Kerswell (2009) showed that the lifetime statistics for puffs (for sufficiently long computational domains) did not change for either constant pressure drop or constant mass flux conditions. Therefore it is valid to compare the present results with those found in experiments and numerical simulations under constant mass flux conditions.

To validate that the pipe is internally smooth, the friction factor was determined by measuring simultaneously the pressure drop and the flow rate. The pressure difference was measured by an inverted U-tube manometer between pressure taps at $625D$ and $1514D$ from the pipe inlet, covering almost $890D$. The first pressure tap was far enough from the entrance to avoid effects due to the development of the flow, even at high Reynolds numbers (the entrance length for $Re = 8000$ is approximately $500D$). The flow rate was determined by measuring the weight of the fluid that exits the pipe over at least 200 seconds. The result for the measured friction factor F as a function of Re is shown in figure 1, in comparison to Poiseuille's law ($F = 64/Re$). A laminar flow state could be sustained for $Re > 9 \times 10^3$, before natural transition occurred. Since experiments are carried out only for $Re < 2000$, it is not expected to observe spontaneous generation of turbulence. Using laser Doppler anemometry (LDA), a velocity profile was measured at $2000D$ from the pipe entrance for $Re = 1750$. Figure 1 shows the measured velocity profile in comparison to a parabolic Poiseuille profile based on the measured flow rate. In the lifetime experiments, the centreline velocity was measured by LDA at the same location to validate that the flow disturbance has the typical characteristics of a puff. This is more reliable than observing the jet angle at the pipe exit (Rotta 1956; Hof *et al.* 2006). After each measurement series, the Reynolds number is determined based on the measured mass flow rate and measured temperature, and could be determined with an estimated total uncertainty of ± 4 (i.e. 0.2 % at $Re = 2000$).

In a lifetime experiment, the fully developed laminar flow is shortly perturbed to create a localized flow disturbance. In the current experiment the flow is disturbed by a zero mass flux disturbance, at $1514D$ from the pipe entrance. The non-dimensional amplitude of the disturbance was equal to 0.1, based on the ratio of disturbance mass flux and pipe-flow mass flux. The amplitude is above the critical amplitude to create a puff (Darbyshire & Mullin 1995; Hof *et al.* 2003). The flow is perturbed during 0.0625 s (1.1–$1.2D/U_b$), which is much shorter than the disturbance time of 10–$20D/U_b$ used in previous experiments (Hof *et al.* 2006, 2008; de Lozar & Hof 2009). Previously, Mullin & Peixinho (2006) found that the critical Reynolds number is reduced by increasing the disturbance amplitude. The amplitude was chosen in correspondence to the lowest critical Reynolds number reported by Mullin & Peixinho (2006). However, de Lozar & Hof (2009) already showed that the type of disturbance did not change the lifetime scaling.

In the present experiment the lifetime of a puff is determined using two differential pressure sensors (Validyne DP45). One pressure transducer (PT_1) measures the pressure drop between taps at $125D$ and $250D$ (S_2) from the disturbance, and the

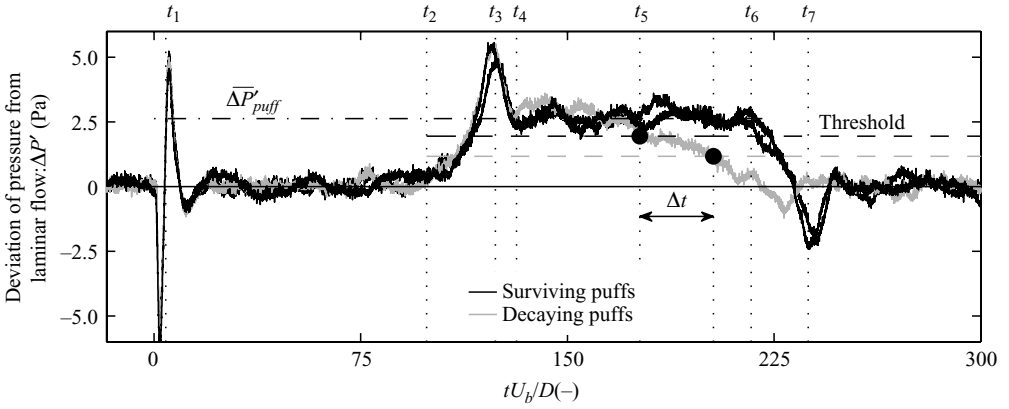

FIGURE 2. Three instantaneous time series of pressure data at $Re = 1822$, measured by PT_1 showing two surviving and one decaying puff. The dashed black line is the threshold level (T_1) used to determine the location of decay, the second (dashed grey line) threshold (T_2) is used to determine the puff disintegration time. See text for details.

second (PT_2) between $250D$ and $496D$ (S_3). Both pressure transducers were calibrated using a micromanometer (Betz) and have a full range of 150 Pa with an accuracy better than 0.75 Pa. In the remainder of this section only the results from the first pressure sensor (PT_1) are shown, but an identical analysis applies to each time series measured for PT_2. The extension to much larger domains by adding more pressure sensors is trivial.

Figure 2 shows three signals recorded by PT_1; for clarity the pressure drop due to laminar flow ($\Delta P \sim 64$ Pa) has been subtracted. The recording starts just before the disturbance is applied at t_1, where the signal shows a single oscillation with a large amplitude. The oscillation ensures that the disturbance was applied. The short-duration pressure oscillation does not induce any significant acceleration or deceleration of the fluid mass in the pipe. The amplitude of the oscillation would be much larger when generated by a non-zero mass flux injection, i.e. when the injected mass is not simultaneously removed.

After the flow has been disturbed, the disturbance forms into a puff and is convected downstream. Since the puff is now present in section S_1, the pressure drop measured by PT_1 is only due to laminar flow, hence the additional pressure drop $\Delta P' = 0$. At t_2 the puff begins to enter section S_2, indicated by the increase in $\Delta P'$, which reaches a maximum at t_3. Then it falls to approximately half the maximum value, which is indicative of an adverse pressure gradient at the transition side of the puff. Rotta (1956) derived that the theoretical upper limit of the pressure *increase* due to the transition from a laminar velocity profile to a uniform velocity profile is equal to $1/3\rho U_b^2$. This would imply a pressure rise of almost 10 Pa. This is not observed in the present data, because the mean velocity profile inside the puff is not uniform. Nevertheless, the predicted adverse pressure gradient is clearly visible.

Figure 2 shows the pressure time series (black lines) for two arbitrary puffs. Both time series show the same characteristics, with a constant additional pressure drop between t_4 and t_6, indicating that the entire puff is inside section S_2. When the puff leaves this section, the same characteristics in pressure are observed as when the puff enters the domain. Due to the presence of only the transition front inside section S_2, a sublaminar pressure drop ($\Delta P' < 0$) is observed around t_7. Hence, both puffs survived

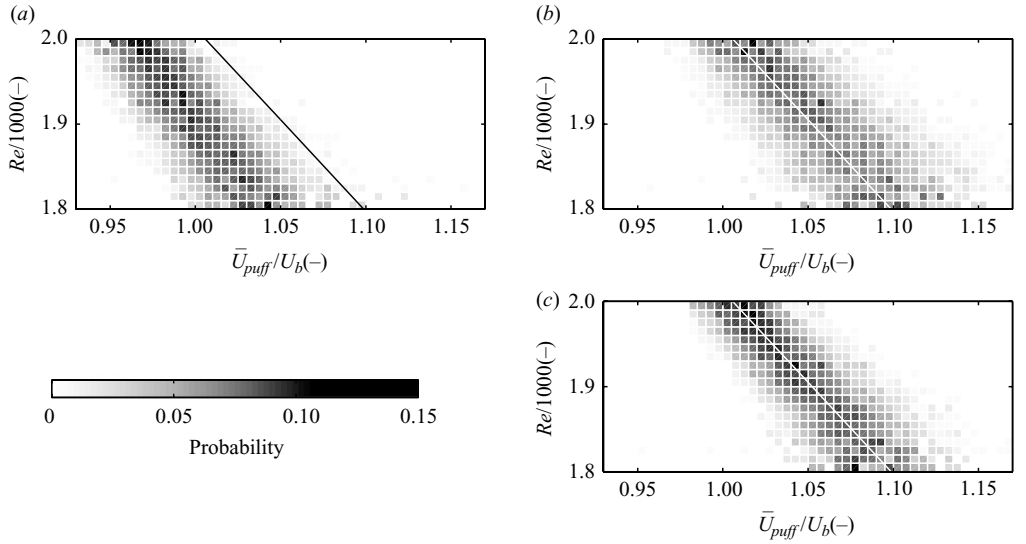

FIGURE 3. Probability density functions of relative average puff velocity as a function of Re; (a) in section S_1; (b) in section S_2; (c) in section S_3. The inclined straight line is a least square fit to the velocity distribution in section S_2 and is given in the other plots for comparison.

while passing section S_2. For the time series represented in light grey the behaviour up to t_5 is the same as previously described. However, for $t > t_5$ the sublaminar pressure difference is not observed, from which it can be concluded that the puff decayed within section S_2.

This allows for the determination of the lifetime of each individual puff by observing the time at which $\Delta P'$ drops below a certain threshold. The threshold value should be chosen below the additional pressure due to the presence of a puff, but should be higher than the noise amplitude of the signal in the absence of a puff. After some preliminary investigation a single threshold value of 1.95 Pa was chosen for all Reynolds numbers (indicated in figure 2). The mean value for $\Delta P'$ between t_4 and t_6 ($\overline{\Delta P'}_{puff}$) was determined for all puffs that survive beyond the downstream pressure tap. A minimum value of $\overline{\Delta P'}_{puff} = 2$ Pa was found. The pressure signal noise fluctuation is estimated at 0.37 Pa for laminar flow, which is less than one-fifth of the selected threshold. The individual lifetimes that were found depended on the selected threshold value, although the result for the scaling of $\tau(Re)$ did not change significantly for threshold values between 1.2 and 2.7 Pa.

In figure 2 it is clearly visible that the sublaminar pressure peak in t_7 does not occur at $t\ U_b/D = 250$, which would be expected when the puff travels with the bulk velocity. This indicates that the puff is not travelling at the bulk velocity, but slightly faster. Given the distance between the pressure taps and the time difference between the occurrence of the pressure peaks, the average velocity of the puff can be determined. Only puffs that survive beyond the last pressure tap (at $496D$ after the injection point) are taken into account. Since hardly any puff survived beyond $496D$ for $Re < 1800$, only the measured mean velocities for $1800 < Re < 2000$ are determined.

Figure 3 shows the probability density function of the mean puff velocity in sections S_1, S_2 and S_3. If puffs would move at a constant mean velocity through the pipe, these figures would be identical. Comparing the graphs in figure 3 shows that the puff first

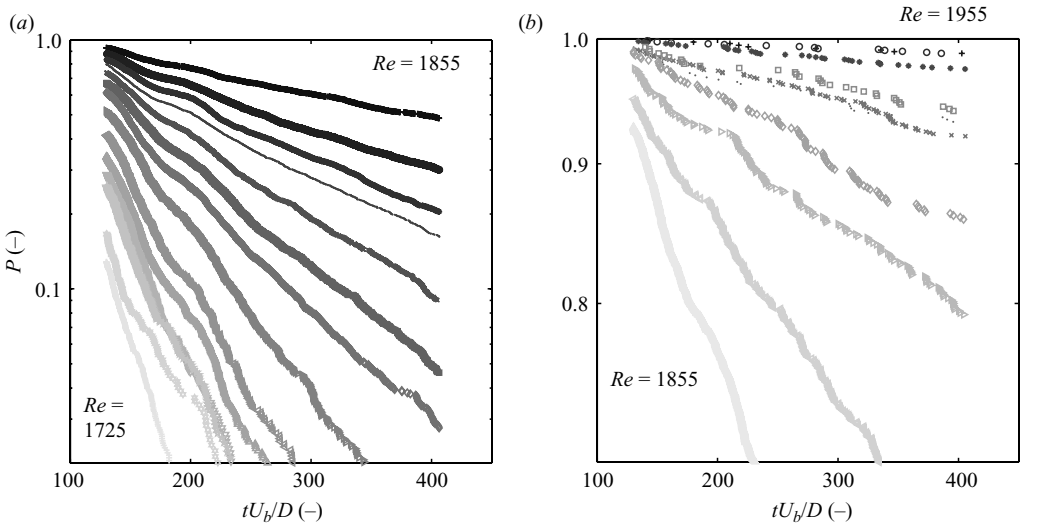

FIGURE 4. Semilog plots of the probability $P(t;Re)$ that a puff survives a time $t\ U_b/D$, where U_b is the bulk velocity and D the pipe diameter, for Re between 1725 ± 5 and 1955 ± 5, in increments of 10. The data for $Re = 1855$ appears in both graphs for reference. The slope of each curve determines $\tau(Re)$ defined in (1), which increases with Re.

accelerates as it moves downstream, while the velocity PDF in sections S_2 and S_3 appear to be identical.

Clearly, the puff velocity at given Re is not fixed. An open question is whether each puff travels at its own constant velocity (for fixed Re), or that the puff velocity is variable as it travels along the pipe. An indication of the validity of the second statement is the correlation coefficient of the puff velocity in sections S_2 and S_3, which turns out to be between 0.49 and 0.51. This implies that the puff velocity is variable.

Note that in earlier measurements (Hof *et al.* 2006, 2008), in which the survival probability was determined for a fixed pipe length L, the characteristic non-dimensional lifetime was determined as $\tau = L/U_{puff}$, where U_{puff} is the mean puff velocity determined from the time difference between the moment of injection and the moment the puff reaches the pipe exit at a distance L. Since the puff velocity is not uniquely defined, we prefer to non-dimensionalize the directly measured lifetime with D/U_b.

3. Results

To determine the characteristic lifetime τ, first the lifetime of each individual puff was determined. Then the measurements were sorted according to their Reynolds number (given by the temperature reading at the pipe exit) and binned with a width of ± 5 for $Re = 1725, 1735, 1745, \ldots, 1955$. The total number of measurements for each Re is between 500 and 3500. The number of puffs that decayed before arriving at the first pressure tap were removed from the data. Next, $P(t;Re)$ is found as the number of surviving puffs over the total number of data, where it drops by one count for each measured lifetime, until the lifetime exceeds the domain covered by the pressure transducers.

In figure 4 the resulting probability distributions are plotted. Each point in this figure represents the measured lifetime of an individual puff. The results for $P(t;Re)$

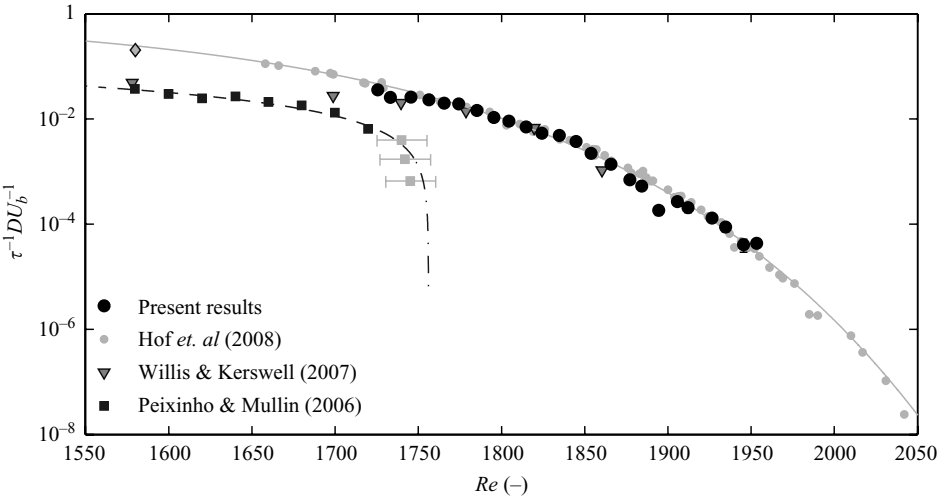

FIGURE 5. The inverse of the characteristic lifetime τ^{-1} as function of Reynolds (Re) number. Data from Peixinho & Mullin (2006) and Hof *et al.* (2008) are included, together with their linear and super-exponential scaling respectively. The data points of Peixinho & Mullin (2006) for $Re \geqslant 1740$ are plotted in light grey since they are, considering the error estimates, measured at the same Reynolds number. The data of Willis & Kerswell (2007*a*) is shown, in which the data point at $Re = 1580$ is reinterpreted (Hof *et al.* 2007; Willis & Kerswell 2007*b*) (Hof *et al.* 2007, (◇), original (▼)).

are clearly exponential (i.e. data follow straight lines in a semilog plot). This is in agreement with the results for $P(t; Re)$ found by Peixinho & Mullin (2006) and Willis & Kerswell (2007*a*). However, here we observe that even for Re above the critical Reynolds numbers of 1750 and 1870 identified by Peixinho & Mullin (2006) and Willis & Kerswell (2007*a*) respectively, numerous puffs decay. Moreover, decaying structures are observed for $Re > 1900$, which is the Reynolds number at which the disturbances were initiated in the experiments by Peixinho & Mullin (2006).

In previous investigations the characteristic lifetime $\tau(Re)$ was obtained by determining the median or half lifetime, i.e. the lifetime for which the survival probability equals 0.5 (Faisst & Eckhardt 2004; Peixinho & Mullin 2006; Willis & Kerswell 2007*a*, 2009). This approach depends heavily on the initial formation time, indicated as t_0 in (1), which is the time needed for the disturbance to develop into a puff. Instead, the characteristic lifetime (together with the formation time t_0) can also be determined by fitting the expression in (1) to the probability distributions in figure 4. This has the advantage that τ can be determined for lifetimes that are shorter than the characteristic lifetime, which avoids the use of a pipe with extremely large values of L/D (Hof *et al.* 2008).

In figure 5 the lifetimes are given based on a least square fit to the probability distribution in figure 4. To estimate the confidence interval a bootstrapping method was used. By extracting 100 000 new data sets of the same length as the initial data set from the data given in figure 4, the median and standard deviation of the best fitting slopes was calculated, resulting in error bars smaller than the symbols used in figure 5. In the same figure also the data of Peixinho & Mullin (2006), Willis & Kerswell (2007*a*) and Hof *et al.* (2008), together with their proposed best fits, are given. Despite the different methods used to determine the lifetimes, the best agreement is found with the data of Hof *et al.* (2008).

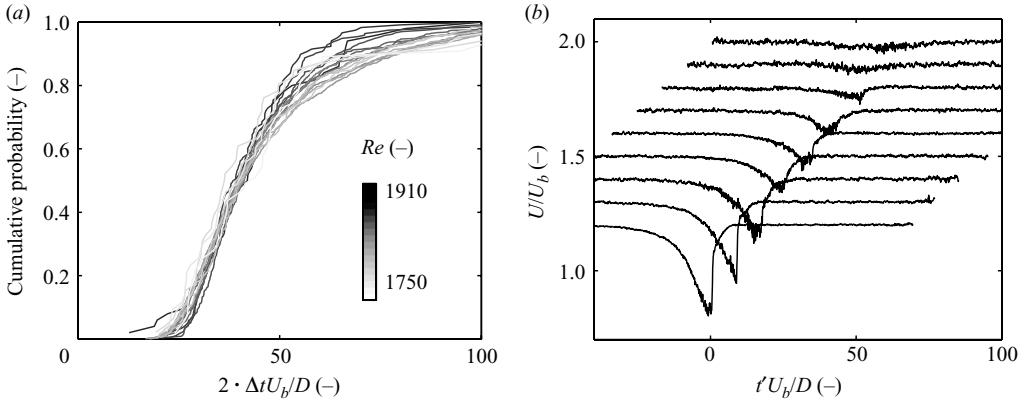

FIGURE 6. (*a*) Cumulative probability distribution of the time needed between initiation and complete decay of a puff; (*b*) Evolution of the conditionally averaged centreline velocity of a decaying puff for nine consecutive times relative to the onset of decay (t_5 in figure 2).

In addition to the measurement of the characteristic lifetime and mean convection velocity of the puffs, we used the pressure measurements to determine the disintegration time ($2\ \Delta t$) of the puffs, which is the time needed to become fully laminar after decay sets in. It is determined from the time between passing a threshold T_1 and a second threshold T_2, and non-dimensionalized by D/U_b (see figure 2). Cumulative probability distributions for the disintegration time were computed for decaying puffs at $Re = 1750, 1760, 1770, \ldots, 1910$, and are plotted in figure 6. No obvious trend with Re is observed, so that the disintegration process seems to be universal over this Re range. It is clear from figure 6 that it takes at least $20D$ for a puff to decay, which is approximately the length of a puff (Wygnanski & Champagne 1973). About 80 % of the puffs need less than $60D$ to disintegrate completely.

To visualize the disintegration itself, the conditionally averaged centreline velocity measured by LDA was used. The pressure measurements are used to determine the location of disintegration with respect to the location of the LDA measurement point. In figure 6 the velocity time series for nine consecutive disintegration times are shown for $Re = 1850 \pm 5$. The top line shows the averaged velocity profile for a puff that started to decay $70D$ upstream of the LDA measurement point. The velocity profiles for the puffs that decay closer to the velocity measurement point are plotted with a vertical offset for clarity. The bottom velocity trace shows the result when a puff has survived up to the point where the velocity is measured and reveals the classical centreline velocity time series observed for a puff.

4. Conclusions

In this paper we present results of direct quantitative measurements for the lifetime of individual localized turbulent structures, or 'puffs', in pipe flow. The mean shape of the puff during decay could be reconstructed from conditionally averaged LDA measurements. Pressure measurements can be used to directly determine the lifetime of each individual puff, where the measurement is based on a predefined threshold for the pressure increase when a puff is present in a given pipe section, rather than a visual inspection of a flow visualization. By combining all measurements, the lifetime probability distribution $P(t; Re)$ is obtained, which shows an exponential decay given in (1), which is characteristic for a memoryless process. By using a fit to the probability

function $P(t; Re)$ the characteristic lifetime $\tau(Re)$ could be determined from the slope of the distribution in a semilog plot. The present results depend neither on the initial formation time t_0, nor on the inclusion of applied disturbances that may fail to develop into a puff. This avoids possible complications of previous investigations of the characteristic lifetime. In addition, we obtained direct measurements of the lifetime probability, rather than observing the probability $P(Re; L)$ that puffs survive a given pipe length L as function of Re, which implicitly assumed an exponential decay for $P(t; Re)$.

The present data confirm that the scaling of the lifetime with Re is super-exponential, as proposed by Hof *et al.* (2008). This confirms that the lifetime does not diverge at a finite critical Reynolds number Re_c within the observed Reynolds number range of $1725 \leqslant Re \leqslant 1955$, which is well above previously reported values for Re_c. For $Re = 1950$ there is a significant fraction of puffs that decay before reaching the end of the measurement domain, with an estimated characteristic lifetime of $25 \times 10^3\ D/U_b$ (see figure 5). This implies that no indication is found for a transition in phase space of the strange saddle into a strange attractor, which would imply a sustained turbulent flow state. Therefore each puff should be considered as a transient flow state. At much higher Reynolds numbers, puffs may split or grow in length to form into 'slugs' (Wygnanski & Champagne 1973; Nishi *et al.* 2008). This behaviour cannot be explained by the current dynamical systems point of view, and a completely different mechanism may describe the transition to turbulence.

In addition, the measurements show that puffs do not move at a constant mean speed through the pipe, which is in contrast with previous observations. Furthermore, the puffs show a rapid decay, which underlies the memoryless process represented by (1), that occurs within 20–70 pipe diameters.

The authors would like to thank Bruno Eckhardt, Marc Avila, Björn Hof and René Delfos for the useful discussions on the work presented here. This work is part of the research programme of the Foundation for Fundamental Research on Matter (FOM), which is financially supported by the Netherlands Organisation for Scientific Research (NWO).

REFERENCES

Darbyshire, A. G. & Mullin, T. 1995 Transition to turbulence in constant-mass-flux pipe-flow. *J. Fluid Mech.* **289**, 83–114.

Eckhardt, B., Schneider, T. M., Hof, B. & Westerweel, J. 2007 Turbulence transition in pipe flow. *Annu. Rev. Fluid Mech.* **39**, 447–468.

Faisst, H. & Eckhardt, B. 2003 Travelling waves in pipe flow. *Phys. Rev. Lett.* **91** (22), 224502.

Faisst, H. & Eckhardt, B. 2004 Sensitive dependence on initial conditions in transition to turbulence in pipe flow. *J. Fluid Mech.* **504**, 343–352.

Hof, B., van Doorne, C. W. H., Westerweel, J., Nieuwstadt, F. T. M., Faisst, H., Eckhardt, B., Wedin, H., Kerswell, R. R. & Waleffe, F. 2004 Experimental observation of nonlinear travelling waves in turbulent pipe flow. *Science* **305** (5690), 1594–1598.

Hof, B., Juel, A. & Mullin, T. 2003 Scaling of the turbulence transition threshold in a pipe. *Phys. Rev. Lett.* **91** (24), 244502.

Hof, B., Lozar, A., Kuik, D. J. & Westerweel, J. 2008 Repeller or attractor? Selecting the dynamical model for the onset of turbulence in pipe flow. *Phys. Rev. Lett.* **101** (21), 214501.

Hof, B., Westerweel, J., Schneider, T. M. & Eckhardt, B. 2006 Finite lifetime of turbulence in shear flows. *Nature* **443** (7107), 59–62.

Hof, B., Westerweel, J., Schneider, T. M. & Eckhardt, B. 2007 Comment on Willis and Kerswell, *PRL* 98, 014501 (2007). *ArXiv:0707.2642* .

Lindgren, E. R. 1969 Propagation velocity of turbulent slugs and streaks in transition pipe flow. *Phys. Fluids* **12** (2), 418–425.

de Lozar, A. & Hof, B. 2009 An experimental study of the decay of turbulent puffs in pipe flow. *Phil. Trans. R. Soc.* A **367**, 589–599.

Mullin, T. & Peixinho, J. 2006 Transition to turbulence in pipe flow. *J. Low Temp. Phys.* **145** (1–4), 75–88.

Nishi, M., Unsal, B., Durst, F. & Biswas, G. 2008 Laminar-to-turbulent transition of pipe flows through puffs and slugs. *J. Fluid Mech.* **614**, 425–446.

Peixinho, J. & Mullin, T. 2006 Decay of turbulence in pipe flow. *Phys. Rev. Lett.* **96** (9), 094501.

Rotta, J. C. 1956 Experimenteller Beitrag zur Entstehung turbulenter Strömung im Rohr. *Ingenieur Archiv* **24**, 258–281.

Wedin, H. & Kerswell, R. R. 2004 Exact coherent structures in pipe flow: travelling wave solutions. *J. Fluid Mech.* **508**, 333–371.

Willis, A. P. & Kerswell, R. R. 2007*a* Critical behaviour in the relaminarization of localized turbulence in pipe flow. *Phys. Rev. Lett.* **98** (1), 014501.

Willis, A. P. & Kerswell, R. R. 2007*b* Reply to comment on 'Critical behaviour in the relaminarization of localized turbulence in pipe flow'. *ArXiv:0707.2684v1* .

Willis, A. P. & Kerswell, R. R. 2009 Turbulent dynamics of pipe flow captured in a reduced model: puff relaminarization and localized 'edge' states. *J. Fluid Mech.* **619**, 213–233.

Wygnanski, I. J. & Champagne, F. H. 1973 Transition in a pipe. Part 1. Origin of puffs and slugs and flow in a turbulent slug. *J. Fluid Mech.* **59**, 281–335.